

PAPER • OPEN ACCESS

A Case Study of Modern Heritage Building: Base Isolation Seismic Retrofit for Preservation of its Architectural Distinguishing Features

To cite this article: Gloria Terenzi *et al* 2020 *IOP Conf. Ser.: Mater. Sci. Eng.* **960** 032056

View the [article online](#) for updates and enhancements.

You may also like

- [Bio-inspired passive base isolator with tuned mass damper inerter for structural control](#)
Haitao Li, Henry T Yang, Isaac Y Kwon et al.
- [Methods for Improving the Seismic Performance of Structures - A Review](#)
Snehansu Nath, Nirmalendu Debnath and Satyabrata Choudhury
- [Development and characterization of a magnetorheological elastomer based adaptive seismic isolator](#)
Yancheng Li, Jianchun Li, Weihua Li et al.



The Electrochemical Society
Advancing solid state & electrochemical science & technology

241st ECS Meeting

May 29 – June 2, 2022 Vancouver • BC • Canada

Extended abstract submission deadline: Dec 17, 2021

Connect. Engage. Champion. Empower. Accelerate.
Move science forward



Submit your abstract



A Case Study of Modern Heritage Building: Base Isolation Seismic Retrofit for Preservation of its Architectural Distinguishing Features

Gloria Terenzi¹, Elena Fuso¹, Stefano Sorace², Iacopo Costoli²

¹Department of Civil and Environmental Engineering, University of Florence, Via S. Marta 3, 50139 Florence, Italy

²Polytechnic Department of Engineering and Architecture, University of Udine, Via delle Scienze 206, 33100 Udine, Italy

gloria.terenzi@unifi.it

Abstract. Several Italian buildings designed by eminent architects and structural engineers in the second half of the 20th century are now included in modern heritage listings. At the same time, as they were designed before the issue of coordinate national Technical Standards, often require important structural rehabilitation interventions. One of the most representative case studies of that period in Florence, i.e. the building now housing the Automobile Club Headquarter and a B&B Hotel, is examined in this paper. A seismic assessment analysis carried out on the structure highlighted strength deficiencies in several members and potentially severe pounding conditions between the two constituting wings of the building, separated by a narrow technical gap. In order to improve the seismic performance without altering the architectural appearance of the building, characterized by large windows in the façades, free internal spaces and elegant proportions of the main structural members, a base isolation retrofit hypothesis is proposed. A substantial seismic improvement is obtained in rehabilitated conditions, as assessed by the achievement of safe stress states for all members up to the basic design normative earthquake level, as well as of maximum relative lateral displacements of the two wings constrained below the technical gap width.

1. Introduction

Italy is a country characterized by an architectural heritage of inestimable value. This also applies to several buildings erected in the second half of the 20th century, designed by eminent architects and structural engineers, some of which are now also included in modern heritage listings. At the same time, these over 60 years-old buildings were designed before the issue of coordinate national Technical Standards, and may require important structural rehabilitation interventions.

One of the most interesting architectural expressions of the early 1960s in Florence, i.e. the building now housing the Automobile Club Headquarter and a B&B Hotel, is examined in this paper as a representative case study of that period. Designed by the Florentine Architect Giuseppe Giorgio Gori, it was built between 1959 and 1961 with a reinforced concrete and steel structure. Among other distinguishing features, it is particularly noticed the presence of “trestles” marking the volume used as offices, to which double cantilevered beams supporting the upper floor of the hotel are connected.



The original design documentation was collected through careful record research, including site images and related technical development documents. A simulated project was carried out for the structural members not detailed in the original design drawings. Detailed on-site surveys were also developed on the building, to evaluate the correlation of the geometrical dimensions of the exposed elements to the design ones.

A seismic assessment analysis carried out on the structure highlighted strength deficiencies in several members, for which stress state checks were not passed starting from the normative basic design earthquake level. Furthermore, potentially severe pounding conditions between the two constituting wings of the building (named Unit 1 and Unit 2 in the following), separated by a narrow technical gap, were evaluated. In order to improve the seismic performance of the building without altering its architectural appearance, characterized by large windows in the façades, free internal spaces and elegant proportions of the main structural members, a base isolation retrofit hypothesis is developed in this study. Due to the irregularities in plan and along the height of the building, Double Concave Sliding Surface (DCSS) devices are adopted for the isolation system.

The architectural and structural characteristics of the building and the results of the time-history assessment analyses in current and retrofitted conditions are discussed in the next Sections.

2. Seismic assessment of Automobile Club Headquarter and B&B Hotel building

A selected number of structural plans of the building is shown in Figures 1 through 3. The A-A and B-B vertical sections of the building, traced out in the plans, are displayed in Figures 4 and 5.

As highlighted by these drawings, the structural system is notably irregular and articulated both in plan and elevation. The technical separation gap between Unit 1 and Unit 2, identified with a dashed blue line in the plans, is equal to 30 mm, i.e. the thickness of the wooden formworks used to cast the columns and the internal perimeter beams of Unit 2 wing situated in front of Unit 1.

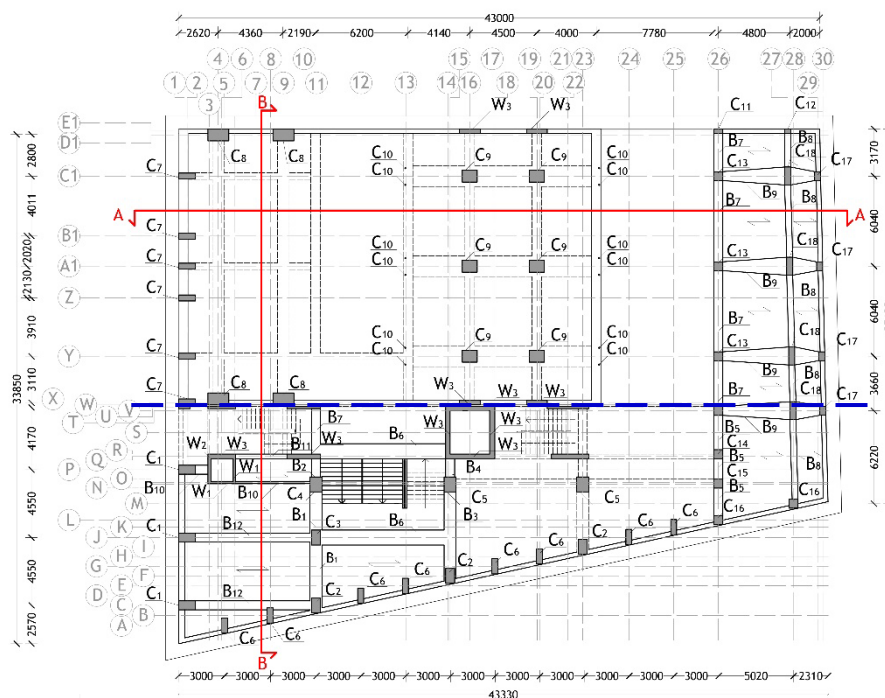


Figure 1. Structural plan of the ground floor (height 0.00 m from ground level)

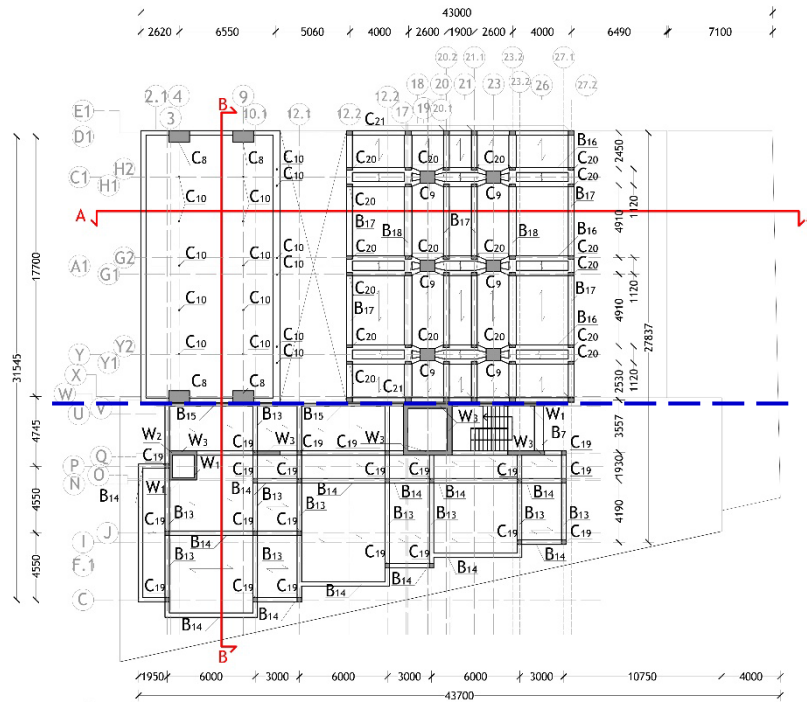


Figure 2. Structural plan of the first complete floor of the hotel (height 11.15 m from ground level)

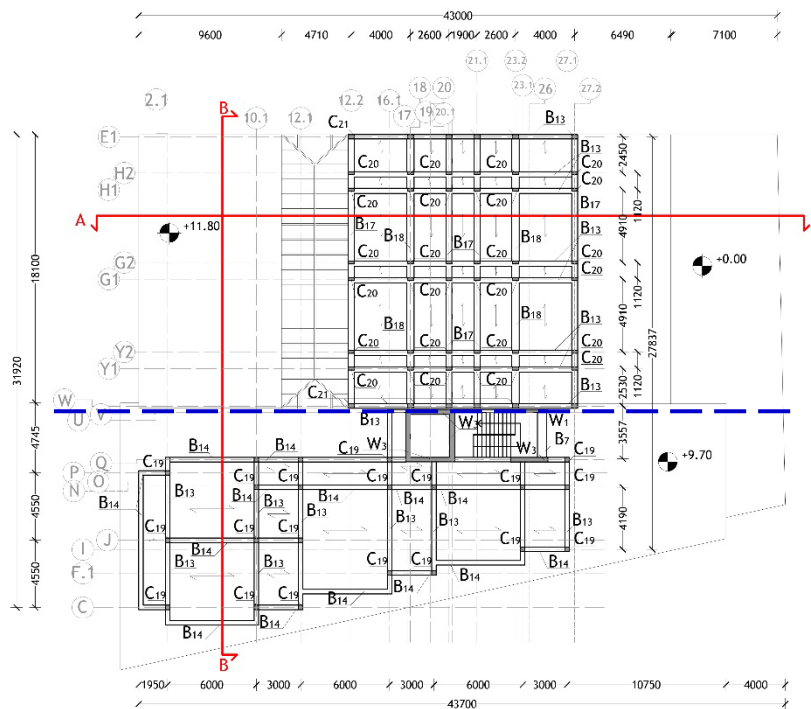


Figure 3. Structural plan of the second and third complete floor of the hotel (heights 14.50 m e 17.85 m from ground level)

Among other peculiarities of the structural system, it is worth mentioning the presence of three wide two-end cantilevered coupled beams in the great hall situated in the main wing of Unit 2, with section height variable from 2250 mm, measured at the external faces of the supporting columns, to 1750 mm,

at the ends. The latter bear the perimeter columns of the above standing columns of the hotel building structure, as well as the underlying mezzanine floors of the same building, suspended to the cantilevered beam ends by a set of $\phi 22$ steel tie-rods incorporated in $\phi 80$ copper fire-protection casings filled with cementitious mortar.

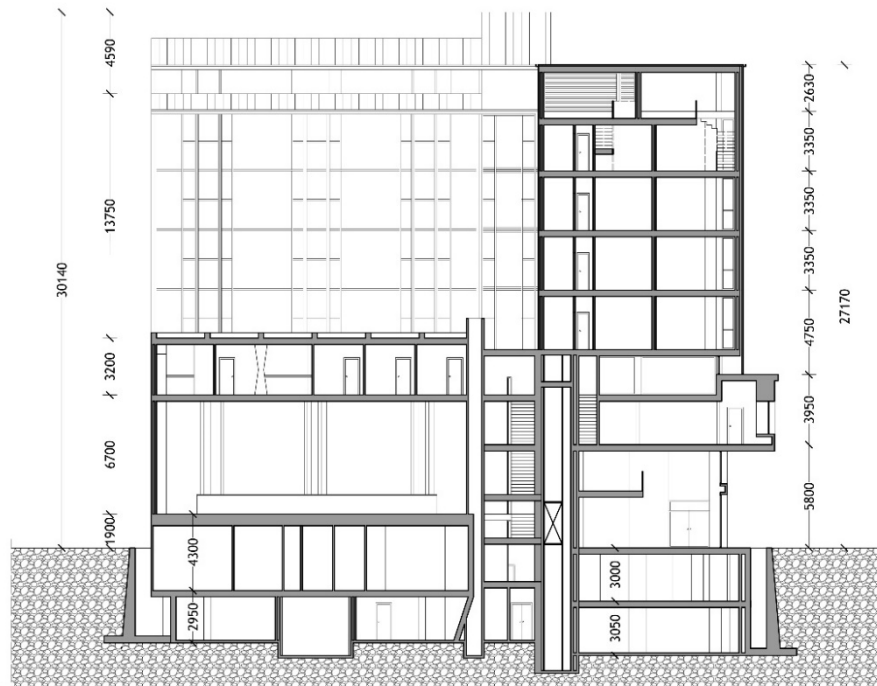


Figure 4. Vertical section of the building denoted as A-A in the structural plans

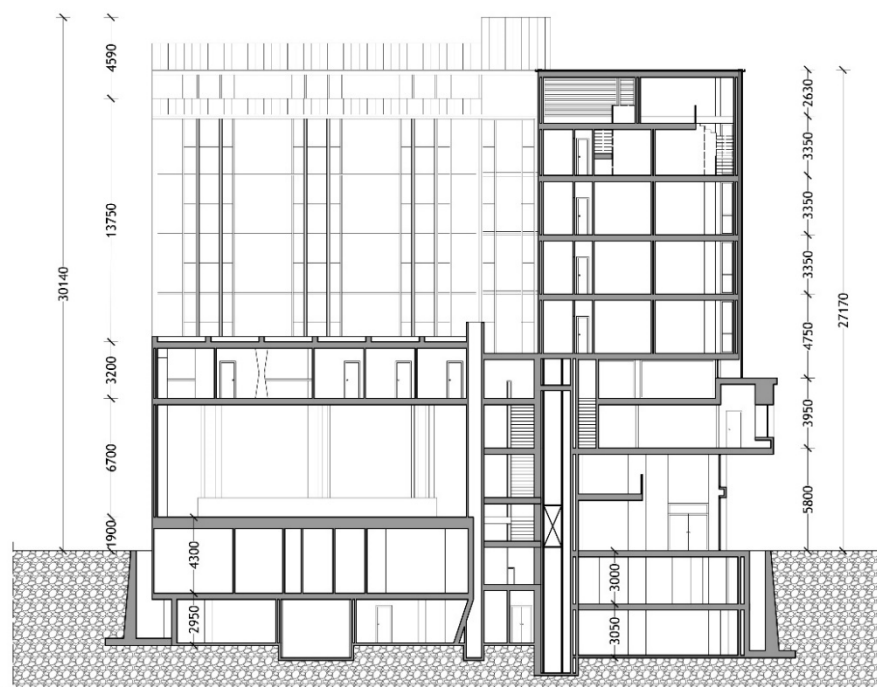


Figure 5. Vertical section of the building denoted as B-B in the structural plans

Although specific diagnostic tests were not carried on the structural system, a careful examination of the original design documentation, integrated by detailed on-site surveys, helped to achieve the highest knowledge level of structural materials and members for the aims of the assessment analysis, named LC3. Consistently with the prescriptions of the Italian Technical Standards [1] and relevant Instructions [2], value 1 was assumed for the “confidence factor”, FC, i.e. the additional knowledge level-related safety coefficient to be introduced in stress state and displacement-related checks.

The following mechanical properties resulted from the technical design relations, site development and final testing documents: mean cubic compressive strength of concrete equal to 25 MPa; yield stress and tensile strength of the reinforcing steel bars equal to 325 MPa and 433 MPa, respectively.

3. Assessment analysis in current conditions

The structural analyses were carried out by the finite element model displayed in Figure 6, generated by the SAP2000NL calculus program [3]. Frame elements were used for the R/C beams and columns, shells for the R/C walls, and cables for the steel tie-rods.

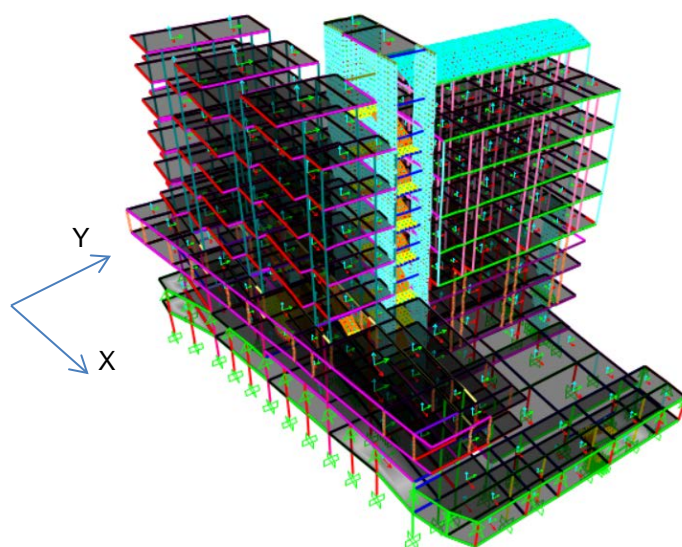


Figure 6. View of the finite element model of the structure

3.1. Modal analysis

The modal analysis of the structure highlights a main translational mode along X of Unit 1, with vibration period of 0.795 s, and Unit 2, with period of 1.072 s; and a main translational mode along Y of Unit 1, with period of 0.989 s, and Unit 2, with period of 1.361 s. Due to the wide geometrical dimensions and the complexity of the model, 30 modes are needed to activate more than 90% of the total seismic mass along X and Y, and a total of 52 modes around Z.

3.2. Time-history and seismic performance assessment analysis

The performance evaluation analysis was carried out for the four reference seismic levels fixed in the Italian Standards [1], that is, Frequent Design Earthquake (FDE, with 81% probability of being exceeded over the reference time period V_R); Serviceability Design Earthquake (SDE, with 63%/ V_R probability); Basic Design Earthquake (BDE, with 10%/ V_R probability); and Maximum Considered Earthquake (MCE, with 5%/ V_R probability) The V_R period is fixed at 75 years, which is obtained by multiplying the nominal structural life V_N of 50 years by a coefficient of use C_u equal to 1.5, imposed to buildings with significant crowding conditions, like the case study one. By referring to topographic category T1 (flat surface), and B-type soil, the resulting peak ground accelerations for the four seismic levels referred to

the city of Florence are as follows: 0.065 g (FDE), 0.078 g (SDE), 0.181 g (BDE), and 0.227 g (MCE). For the development of the time-history analyses, two families of seven accelerograms were generated from the pseudo-acceleration elastic response spectra referred to Florence, plotted in Figure 7. In each analysis, the accelerograms were applied in groups of two simultaneous horizontal components, with the first one selected from the first generated family of seven motions, and the second one selected from the second family.

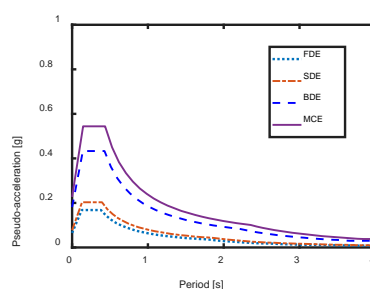


Figure 7. Normative pseudo-acceleration elastic response spectra for Florence and the reference site parameters

For brevity's sake, the results of the analysis are synthesized in terms of maximum stress states in the structural elements and maximum relative displacement of the upper storey floors of the two Units at the BDE.

The stress state checks show generalized unsafe response conditions of columns and beams, with unsafety factors reaching nominal values up to about 5. By way of example of the response of a Unit 2 column (belonging to the family named “C20” in the structural plans of Figures 1 through 3), the $M_{Ic,1}$ – $M_{Ic,2}$ biaxial moment interaction curves (being $M_{Ic,1}$, $M_{Ic,2}$ the bending moments around the local axes 1 and 2 of columns in plan, with 1 parallel to X, and 2 to Y) graphed by jointly plotting the two bending moment response histories obtained from the most demanding among the seven groups of BDE-scaled ground motions, are plotted in Figure 8. The boundary of the $M_{Ic,1}$ – $M_{Ic,2}$ safe interaction domain of the column, traced out for the value of the axial force referred to the basic combination of gravity loads, is also shown in the graph. For this column, the response curves highlight maximum $M_{Ic,1}$ – $M_{Ic,2}$ combined values about 4.5 times greater than the corresponding values situated on the safe domain boundary, denoting the most critical conditions with respect to the weak axis (i.e. axis 1).

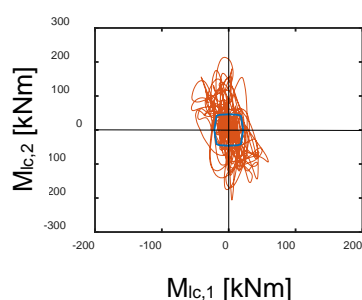


Figure 8. $M_{Ic,1}$ – $M_{Ic,2}$ interaction curves for a C20-type column obtained from the most demanding BDE-scaled group of input accelerograms

The relative displacement time-history of the upper storey floors of the two Units, situated at a height of 24.45 m from the ground level — obtained as the difference of the displacement histories of the same floors — for the same group of BDE-scaled accelerograms which Figure 8 is referred to, are visualized

in Figure 9. Although pounding was not expressly modelled in the analysis, the response in terms of mutual displacements clearly underlines the possibility of high collisions between the two wings of the building, which could cause severe local damages in structural members facing the existing separation gap, in addition to a considerable increase of the already markedly unsafe stress states of columns and beams, and particularly of those situated in the upper storeys near to the gap alignment.

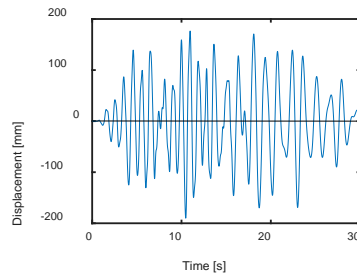


Figure 9. Relative displacement time-history of the upper storey floors of the two Units obtained from the most demanding BDE-scaled group of input accelerograms

The results of the assessment analysis prompted to adopt a retrofit strategy capable of substantially improving the poor performance evaluated in current conditions and at the same time, not impairing the architectural value of the building, as discussed in the next Section.

4. Base isolation retrofit hypothesis

As mentioned above, by considering the irregularities in plan and along the height of the building, DCSS devices were adopted for the isolation system. Indeed, thanks to this choice, the performance of the latter results to be independent of the structural characteristics of the superstructure [4]. The isolators were incorporated at the foot of each column and below the bottom slabs of the two elevator pits.

4.1. Design of the isolation system

The DCSS isolators were designed by complying with the multi-step procedure presented in [5] and applied to several different seismic retrofit designs [6-11], summarized herein. The first step consists in fixing the vibration period T_d of the isolator in dynamic response conditions (i.e. the period associated with the second-branch stiffness of the reference response cycle of the device, k_d). A rounded value of 3 s — typical of the smallest DCSS devices in standard production — can be tentatively assumed for T_d . Then, by referring to the schematic cross section of a DCSS device and the geometrical parameters of one of the two equal sliding surfaces sketched in Figure 10, where R =radius of each curved surface, h =slider centre-to-surface distance (i.e. the distance between the “pivot point” P of the articulated slider and the face of each spherical surface) and $R-h$ the effective pendulum length of each sliding surface, the tentative value of the effective double pendulum length $L_{DCSS}=2 \cdot (R-h)=2R-2h$ is deduced from the T_d expression:

$$T_d = 2\pi \sqrt{\frac{L_{DCSS}}{g}} \quad (1)$$

where g is the acceleration of gravity, resulting in:

$$L_{DCSS} = \frac{T_d^2}{4\pi^2} g \quad (2)$$

The friction coefficient μ is fixed at step 2. The standard manufacturing value $\mu=0.025$ is adopted for this case study, where high friction effects — required to remarkably constrain lateral displacements — are unnecessary, as both Unit 1 and Unit 2 are not adjacent to other buildings. Afterwards, a tentative

value of the maximum isolator displacement, d_{max} , must be selected. For applications in medium seismicity zones, like Florence, $d_{max}=\pm 200$ mm is generally enough to meet the displacement demand up to the MCE level with considerable safety margins.

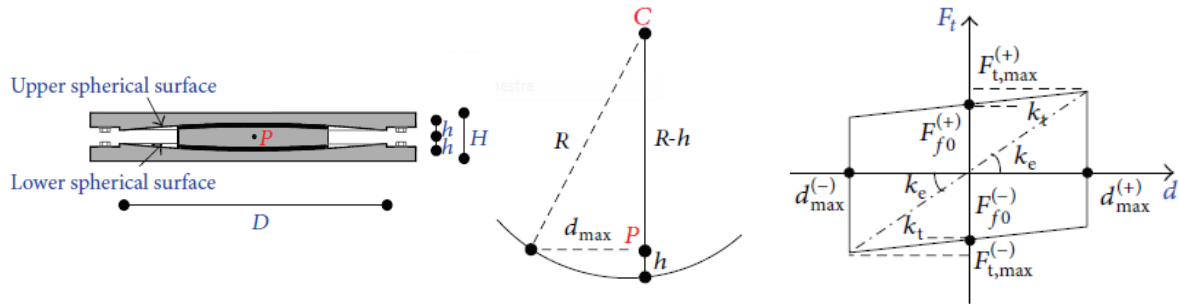


Figure 10. Schematic cross section, geometrical parameters and response cycle of a DCSS isolator

Based on the selected μ and d_{max} values, the equivalent vibration period T_e of the isolator, associated with the “linear equivalent” (or “secant”) stiffness, k_e , and the equivalent viscous damping coefficient ratio, ξ_e , are calculated with the following expressions:

$$T_e = 2\pi \sqrt{\frac{1}{g \left(\frac{1}{L_{DCSS}} + \frac{\mu}{d_{max}} \right)}} \quad (3)$$

$$\xi_e = \frac{2}{\pi} \cdot \frac{1}{\frac{d_{max}}{\mu L_{DCSS}} + 1} \quad (4)$$

Using T_e and ξ_e , in step 3 the maximum spectral displacement at the MCE, $d_{s,MCE}(T_e, \xi_e)$ can be computed, so as to check whether this maximum displacement estimate is lower than the assumed displacement capacity d_{max} . To this aim, the normative displacement spectrum at linear viscous damping ratio $\xi=5\%$ is scaled by ξ_e , and the ξ_e -scaled spectrum is entered with T_e , obtaining $d_{s,MCE}(T_e, \xi_e)$ in output. If the check $d_{s,MCE}(T_e, \xi_e) \leq d_{max}$ is passed, the tentative pendulum geometry of the isolator is confirmed.

The application of the procedure, for $\mu=0.025$ and $d_{max}=\pm 200$ mm, induced to the select from the manufacturer’s catalogue [12] isolators characterized by L_{DCSS} equal to 3100 mm for all columns and the two elevator pits. Based on the calculated values of the maximum axial force acting on the vertical members, the D diameters of the adopted devices range from 490 mm to 540 mm.

4.2. Time-history final verification analysis

A general view and a detail of the finite element model of the structure incorporating the DCSS isolators are shown in Figure 11. The results of the final verification analysis carried out by this model are synthesized in Figures 12 and 13, which duplicate, for retrofitted conditions, the graphs in Figures 8 and 9 above.

The $M_{Ic,1}-M_{Ic,2}$ biaxial moment interaction curves of the C20-type column referred to in Figure 8, highlight that the response is reduced by a factor about equal to 10 thanks to the protective action of the base isolation system. This helps to constrain the response curves within the boundary of the $M_{Ic,1}-M_{Ic,2}$ safe interaction domain, widely exceeded in current conditions. The relative displacement time-history of the upper storey floors of the two Units is reduced by a factor approximately equal to 10 too, with maximum values neatly below the width of the existing separation gap. Although without expressly

modelling pounding in this analysis, this result highlights that the mutual collisions between the constituting wings of the building are prevented in the rehabilitated configuration.

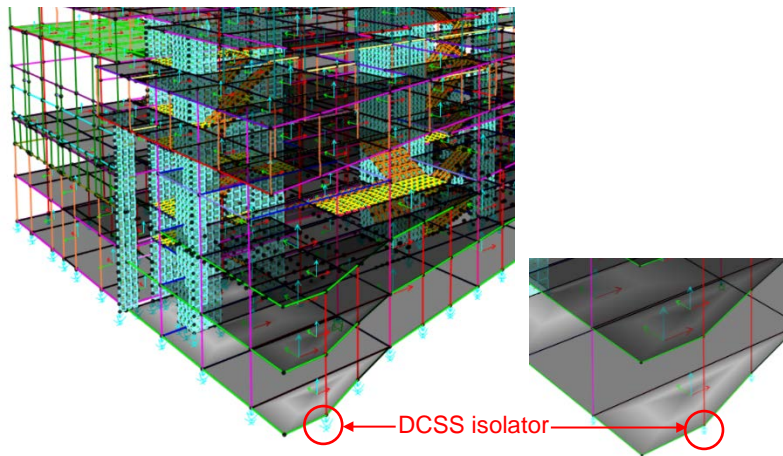


Figure 11. Views of the finite element model of the structure incorporating the base isolation system

The $M_{Ic,1}$ – $M_{Ic,2}$ biaxial moment interaction curves of the C20-type column referred to in Figure 8, highlight that the response is reduced by a factor about equal to 10 thanks to the protective action of the base isolation system. This helps to constrain the response curves within the boundary of the $M_{Ic,1}$ – $M_{Ic,2}$ safe interaction domain, widely exceeded in current conditions.

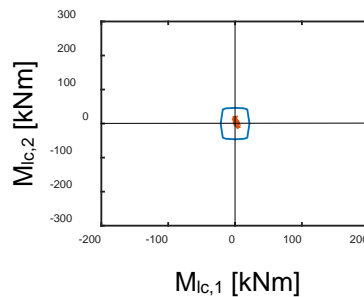


Figure 12. $M_{Ic,1}$ – $M_{Ic,2}$ interaction curves for a C20-type column obtained from the most demanding BDE-scaled group of input accelerograms in base isolated conditions

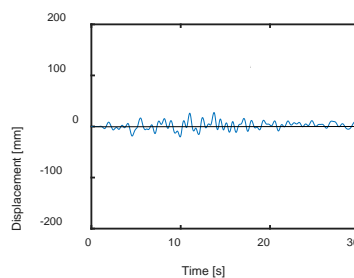


Figure 13. Relative displacement time-history of the upper storey floors of the two Units obtained from the most demanding BDE-scaled group of input accelerograms

The benefits of the retrofit intervention are extended to all members, which meet the stress state checks at the BDE level of seismic action. Furthermore, consistently with the substantial reduction of the lateral displacements of the two Units, the maximum inter-storey drifts are shifted below the Immediate Occupancy performance level-related drift limit of 0.33% of the storey heights, which allows preventing damage to infills and the other drift-sensitive non-structural elements of the building. The maximum displacements of the DCSS isolators at the MCE level result to be no greater than 100 mm, i.e. half the available device displacements of ± 200 mm, definitely validating their design choice.

5. Conclusions

The seismic assessment analysis carried out on the case study structure highlighted generalized unsafe stress states in the columns and beams of the frame skeleton, as well as in special elements, like the suspension tie-rods of Unit 2 the mezzanine floors. Remarkable potential pounding conditions between the two Units were also evaluated. The base isolation retrofit hypothesis proposed in this study allows reaching a substantial improvement of the seismic response surveyed in current conditions, in terms both of maximum stress states, constrained within the elastic domain limits of all members, and lateral displacements, shrunk below the width of the separation gap of the two wings. At the same time, this retrofit strategy does not cause any intrusion in the building, preserving its high architectural quality.

Acknowledgment(s)

The study reported in this paper was sponsored by the Italian Department of Civil Protection within the ReLUIIS-DPC Project 2019/2021 – Work Package 15: Normative Contributions for Isolation and Dissipation. The authors gratefully acknowledge this financial support.

References

- [1] Italian Council of Public Works, “Technical Standards on Constructions,” *Italian Council of Public Works*: Rome, Italy, 2018.
- [2] Italian Council of Public Works, “Commentary on the Technical Standards on Constructions,” *Italian Council of Public Works*: Rome, Italy, 2019.
- [3] SAP2000NL, “Theoretical and Users’ Manual, Release 20.07,” *Computers & Structures Inc.*: Berkeley, CA, USA, 2019.
- [4] D.M. Fenz, and M.C. Constantinou, “Behaviour of the double concave friction pendulum bearing,” *Earthquake Engineering and Structural Dynamics*, vol. 35, pp. 1403–1424, 2006.
- [5] S. Sorace, and G. Terenzi, “A viable base isolation strategy for the advanced seismic retrofit of an R/C building,” *Contemporary Engineering Sciences*, vol. 7, pp. 817-834, 2014.
- [6] C. Mori, S. Sorace, and G. Terenzi, “Seismic assessment and retrofit of two heritage-listed R/C elevated water storage tanks,” *Soil Dynamics and Earthquake Engineering*, vol. 77, pp. 123-136, 2015.
- [7] S. Sorace, and G. Terenzi, C. Bitossi, and E. Mori, “Mutual seismic assessment and isolation of different art objects,” *Soil Dynamics and Earthquake Engineering*, vol. 85, pp. 91-102, 2016.
- [8] S. Sorace, and G. Terenzi, “Analysis and seismic isolation of an older reinforced concrete vaulted building,” *Contemporary Engineering Sciences*, vol. 9, pp. 1201-1215, 2016.
- [9] G. Terenzi, and E. Rossi, “Seismic analysis and retrofit of the oldest R/C elevated water tank in Florence,” *Bulletin of Earthquake Engineering*, vol. 16, n. 7, pp. 3081-3102, 2018.
- [10] S. Sorace, G. Terenzi, and I. Costoli, “Base isolation strategy for seismic retrofit of water tanks with shaft staging,” *International Journal of Civil Engineering and Technology*, vol. 9, pp. 891-902, 2018.
- [11] G. Terenzi, S. Sorace, P. Spinelli, and E. Rossi, “Seismic protection of a historical R/C elevated water tank by different base-isolation systems,” *Ingegneria Sismica – International Journal of Earthquake Engineering*, vol. 36, n. 2, pp. 137-157, 2019.
- [12] FIP. Anti-seismic devices product division. [Online] 2019 [Accessed 22. 01. 2020]. Available at <http://www.fip-group.it>.